Human megakaryocytic microparticles induce *de novo* platelet biogenesis in a wild-type murine model

Short Title: Mk microparticles induce platelet biogenesis

Christian Escobar³, Chen-Yuan Kao,^{1,2} Samik Das^{1,2} and Eleftherios T. Papoutsakis^{1,2,3}

¹Department of Chemical and Biomolecular Engineering, ²Delaware Biotechnology Institute and

³Department of Biological Sciences, University of Delaware, Newark, DE 19711

Corresponding Author: Eleftherios Terry Papoutsakis

Address: 15 Innovation Way, Delaware Biotechnology Institute, Newark, DE 19711

Email: epaps@udel.edu **Telephone:** 302-831-8376 **Fax:** 302-831-4841

Word Count (Text): 5295 Word Count (Abstract): 241

Figure Count: 5
Table Count: 2
Reference Count: 42

Key Points

- 1. HuMkMPs target and program megakaryocytic differentiation of muHSPCs in vitro.
- 2. Intravenous administration of huMkMPs enables *de novo* platelet biogenesis *in vivo*.

Abstract

Platelet transfusions are used to treat idiopathic or drug-induced thrombocytopenias. Platelets are an expensive product in limited supply, with limited storage and distribution capabilities due to the inability to freeze them. We have previous demonstrated that, in vitro, megakaryocytic microparticle (huMkMPs) target human CD34⁺ hematopoietic stem & progenitor cells (huHSPCs) and induce their megakaryocytic differentiation and platelet biogenesis in the absence of thrombopoietin. Here, we show that, in vitro, huMkMPs can also target murine HSPCs (muHSPCs) to induce them to differentiate into megakaryocytes in the absence of thrombopoietin. Based on that, using wild-type Balb/c mice, we demonstrate that intravenously administering 2×10⁶ huMkMPs trigger *de novo* murine platelet biogenesis to increase platelet levels up to 49%, 16 hours post administration. huMkMPs also largely rescue low platelet levels in mice with induced thrombocytopenia, 16 hours post administration, by increasing platelet counts by 51% compared to platelet counts in thrombocytopenic mice. Normalized on a tissuemass basis, biodistribution experiments show that MkMPs largely localized to the bone marrow, lungs and liver 24 hours post huMkMP administration. Beyond the bone marrow, CD41⁺ (megakaryocytes and Mk-progenitor) cells were quite frequent in lungs, spleen and especially liver. In the liver, infused huMKMPs colocalized with Mk progenitors and muHSPCs, thus suggesting that huMkMPs interact with muHSPCs in vivo to induce platelet biogenesis. Our data demonstrate the potential of huMkMPs, which can be stored frozen, to treat thrombocytopenias and as effective carriers for in vivo, target-specific cargo delivery to HSPCs.

Introduction

Megakaryocytes (Mks) are large polyploid (≥8N) cells derived from hematopoietic stem and progenitor cells (HSPCs; contained within the CD34⁺-cell compartment), which upon maturation under the action of thrombopoietin (TPO), shed pre/pro-platelets (PPTs) and platelet-like particles (PLPs), which mature quickly into platelets. ¹⁻³ Mks also shed CD41⁺CD42b⁺CD62P⁻ Mk Microparticles (MkMPs). ^{4,5} Cell-derived microparticles/microvesicles (MPs/MVs) are submicron-size extracellular vesicles that are emerging as potential therapeutic agents. ^{6,7} It has been known since 2009 that MkMPs are the most abundant MPs in circulation, and that they are distinct from platelet derived MPs (PMPs). ⁵

In Transfusion Medicine, platelets are an expensive product in limited supply due to the collection and processing steps from donated blood and the inability to freeze them⁸. In the US alone, there are 2.4M platelet doses (3–6x10¹¹ platelets each) administered at a cost of ca. \$524 per dose. As they cannot be frozen, platelets have a useful life of 4-5 days. As a result, they are not easily available in remote locations. Also, there is the possibility of bacterial or viral contamination of platelet products from blood collections ⁹. Thus, a safe, manufactured product that can substitute for platelets and that can be kept frozen is most desirable. Culture-derived platelets hold a great potential for providing an abundant platelet supply^{10,11}, but many problems remain¹². In addition to platelet transfusions, there is a need to enhance platelet biogenesis in patients with thrombotic deficiency (such as is encountered during the treatment of cancer⁸) or excessive bleeding due to trauma.

We have previously shown that human MkMPs (huMkMPs; which can be stored frozen without loss of function¹³) specifically target human CD34⁺ HSPCs (huHSPCs) *in vitro*, leading to fate modification of huHSPCs towards megakaryocytic differentiation in the absence of TPO

^{4,13}. Specifically, co-culture of MkMPs with huHSPCs lead to formation of mature Mks displaying characteristic PPT structures and synthesizing both alpha- and dense-granules without exogenous TPO ^{4,13}. Based on these findings, we hypothesized that huMkMPs are able to maintain their *in vitro* biological activity *in vivo*, and can thus serve as potential therapeutic agent in Transfusion Medicine. To pursue this hypothesis, here, we first demonstrate that, *in vitro*, huMkMPs can target murine HSPCs (muHSPCs) to trigger murine megakaryocytic differentiation. Using in a wild-type murine model, we further demonstrate that infusion of huMkMPs promotes *de novo* murine platelet biogenesis, and can ameliorate antibody-induced murine thrombocytopenia.

Materials and Methods

Several, previously detailed, experimental procedures can be found in Supplemental Materials & Methods. They include: Chemicals and Reagents; *in vitro* human megakaryocyte (Mk) culture derived from mobilized peripheral blood (MPB) CD34⁺ HSPCs; and isolation of human Megakaryocytic Microparticles (huMkMPs).

Isolation of murine hematopoietic stem/progenitor cells (muHSPCs)

All procedures involving mice were approved by the University of Delaware (UD) Institutional Animal Care and Use Committee and are in agreement with the guide for the care and use of laboratory animals¹⁴. All mice were housed with day/night stimulation at UD's Animal Facility, with access to food and water. 4-6-weeks old female Balb/c mice (Jackson Laboratory) were euthanized via CO₂ asphyxiation followed by cervical dislocation to confirm death. Mice were prepared for organ collection by spraying with 70% ethanol. Femurs were extracted and placed in RPMI 1640X (Thermo) with 10% FBS and 1% Antibiotic-Antimycotic (Thermo) to prevent

neutrophil activation. Femurs were decontaminated by triple washes with PBS containing 1% Antibiotic-Antimycotic. Once decontaminated, femur epiphyses were cut and flushed with RPMI 1640X using a 20G needle attached to a 12cc syringe. The effluent was collected and passed through a pre-separation filter (30 microns, Miltenyi). This process continued until the bone appeared white in color on the surface, indicating the bone is empty.

Next, cells were collected at 300 g centrifugation for 10 minutes, followed by red blood cell (RBC) depletion with the treatment of ACK buffer (0.15 M NH₄Cl, 10 mM KHCO₃, 0.1 mM Na₂EDTA, pH 7.2–7.4) for 5 minutes at 4°C ¹⁵. After that, cells were washed twice with PBS (containing 1% Antibiotic- Antimycotic). To isolate murine hematopoietic stem & progenitor cells (muHSPCs), lineage cells were depleted using the Lineage Depletion Kit (Miltenyi), following the manufacturer's protocol.

Co-culture of muHSPCs with huMkMPs

Co-culture of huMkMPs and muHSPCs was perform in a 24-well Transwell plate for enhancing the interaction between huMkMPs with muHSPCs. Transwell membrane insert (Costar, #3470) was inserted into a well with 750 µL of growth medium (IMDM, 20% BIT, 50 ng/ µL of hSCF) in the absence of TPO at the bottom compartment. 60,000 muHSPCs in 200 µL IMDM were seeded onto the membrane insert. After 20 minutes, huMkMPs were added onto the membrane at a ratio of 30 huMkMPs per muHSPC. Both short-term (3-5 hours) or long-term (5 days) co-cultures were performed.

For short-term co-cultures, huMkMPs were pre-stained with the lipophilic dye PKH26 and cytosolic dye CFSE. After 3 or 5 hours of co-culture, cells were harvested, and huMkMPs uptake by muHSPCs was examined via confocal microscopy (Zeiss LSM880).

For long-term co-cultures, cells were cultured for 24 hours in Transwell plate¹⁶ for 24 h, followed by transferring to the lower compartment of the plate. muHSPCs without huMkMP addition served as vehicle control, while muHSPCs cultured in medium supplemented with 50 ng/mL of human TPO served as positive control. At day 5, some cells were harvested for CD41 and ploidy flow-cytometric analysis¹⁵; some other cells were stained with anti-CD41 antibody for live-cell confocal microscopy. Some cells were fixed and stained for beta-tubulin I (TUBB1), von Willebrand factor (vWF), and nucleus (DAPI) imaging, as described⁴. Images were acquired using a ZEISS LSM 880 multiphoton confocal microscope.

Chinese Hamster Ovary (CHO) cell-derived empty vesicles (CHO-MVs)

CHO-MVs were generated from CHO membranes using the protocol of Fang *et. al.*, which yields uniform membrane vesicles with minimal loss to membrane functionality^{17,18}. Briefly, CHO cells were collected from a standard CHO culture¹⁹ at day 2, were stained with PKH26 and lysed with a Dounce homogenizer (Kimble) and hypotonic lysis buffer with protease inhibitor (p8340, Sigma). PKH26-stained cell membranes were isolated using differential ultracentrifugation. The final membrane pellet was resuspended in 700 ul filtered PBS and extruded through a 400-nm polycarbonate membrane (Avanti Lipid Extruder) at 55°C. The concentration of extruded CHO-MVs was quantified using flow cytometry as for MkMPs⁴.

Murine experiments: in vivo impact of intravenously injected huMkMPs

We chose to use 4-6 weeks old female Balb/c mice, since the variation of platelet levels of female mice is smaller than in male mice ²⁰. This would allow to reach statistical significance of the data faster. To evaluate the biological effectiveness of huMkMPs, huMkMPs were injected

into untreated mice or mice treated to induce thrombocytopenia. For untreated mice, 2×10^6 , 6×10^6 huMkMPs, or 6×10^6 CHO-MVs in 100 μ L saline or saline only were injected intravenously via the tail vein. CHO-MVs were used as an additional control. 72-hour post huMkMP injection, $10~\mu$ L of blood was collected retro-orbitally, and platelet counts were measured by flow cytometry: platelets were gated using the forward-scatter and side-scatter gates and standardized using microbeads ($0.2~\mu$ m to $1.34~\mu$ m). The gating was confirmed utilizing FITC rat anti-mouse CD41(BD 553848) to distinguish between noise and platelet events. Control experiments confirmed that platelet counting is not affected by the presence of huMkMPs.

In another set of experiments, $6x10^6$ PKH26-labeled huMkMPs, or saline control were administrated into BALB/c mice. Tissue including bone marrow (BM), lung, liver, and spleen were collected after 4 hours for single-cell isolation²¹ followed by RBC depletion. Harvested cells were stained with anti-CD41 antibody, anti-CD117, or anti-CD45 and analyzed via flow cytometric analysis.

To induce thrombocytopenia, LEAF rat anti-mouse CD41 antibody (MWReg30, Biolegend), at the dose of 1 μg per g murine body weight, was injected once intraperitoneally to induce thrombocytopenia²². Eight hours post-antibody injection, mice (untreated or thrombocytopenic) received 2×10⁶ huMkMPs in 100 μL saline or saline only via intravenous tail-vein injection. 10 μL of blood was collected retro-orbitally, and platelet counts were measured by flow cytometry 24-hour post-antibody-injection. Reticulated-platelet levels were measured as described²², using a thiazole orange assay (BD Retic-Count).

Biodistribution experiments

10⁶ PKH26-stained huMkMPs or CHO-MVs in 100 μL saline (PBS) were injected intravenously into the tail vein of the mice along with saline-only controls. Four hours post injection, 1 mouse from the control group and 3 mice from the huMkMP-injected group were euthanized through CO₂ asphyxiation and the following tissues were surgically excised from each mouse: blood, bone marrow (BM)/femur, brain, heart, kidney, liver, lung, and spleen. The net weight of each mouse and all tissues, except blood, were recorded and tissues were stored in 3-mL of PBS on ice. This procedure was repeated with mice collected 24-hours post injection of huMkMP, CHO-MV, or saline-only control. All tissues were processed within 24 hours of collection. Each tissue, except for blood, was lysed and homogenized with a coarse Dounce homogenizer in 1.5 mL of hypotonic lysis buffer (20 mM Tris-HCL, 10 mM KCl, 2mM MgCl2, 0.5% v/v p8340 protease inhibitor, pH: 7.5). 200 µL of each tissue homogenate were added to a well of a black, opaque 96-well plate, and absolute fluorescence levels was measured with a SpectraMax i3x plate reader (excitation: 547-nm). Fluorescence levels of each tissue from treated mice were assessed as the difference between the absolute fluorescence of experimental mice and fluorescence from tissues of control mice (saline). These values were normalized by (a) overall tissue weight and (b) tissue weight as a fraction of the mouse weight. Normalization by tissue weight accounted for tissuespecific weight variation within each mouse. Mean fluorescence intensity (MFI) of each tissue was divided by their respective tissue mass (weight) to yield MFI per g tissue mass.

Statistical analysis

Data are presented as mean \pm standard error of mean (SEM). Unpaired Student's t test of all data was performed. Statistical significance is defined as *p < 0.05, **p < 0.01, ***p < 0.001.

Results

In vitro, human megakaryocytic microparticles (huMkMPs) target murine hematopoietic stem & progenitor cells (muHSPCs) and induce their megakaryocytic differentiation and expansion in the absence of thrombopoietin

We have previously shown that, in vitro, huMkMPs induce and promote Mk differentiation of huHSPCs without stimulation by TPO, whereby the resulting Mks formed functional PPTs synthesizing both alpha and dense granules⁴. Later, we showed that huMkMPs target only huHSPCs and no other physiologically or ontologically related cells¹³. Here, to test if huMkMPs target and induce muHSPCs to differentiate into murine Mk cells, we first examined uptake of huMkMPs by muHSPCs via short-term co-cultures. We generated huMkMPs from day-12 primary Mk cultures started with frozen, human MPB CD34⁺ cells as described ^{4,13}. huMkMPs were stained with CFSE, a green cytosolic dye staining surface and cytosolic proteins by covalently binding to amines, and PKH26, a lipophilic, membrane-staining dye, and were cocultured with muHSPCs. Confocal-microscopy images were acquired at multiple z planes aiming to determine if huMkMPs recognize, attach to and are possibly internalized by muHSPCs. We examined 70 cells at different time points to capture different stages on interactions between huMkMPs and muHSPCs. huMkMPs recognized, targeted and attached to muHSPCs after 3 hours of co-culture (Fig. 1A), and were taken up by muHSPCs within 5 hours (Fig. 1B). At 3 hours, at all z planes, several stained huMkMPs appear attached to muHSPCs (red arrows), and some were possibly just internalized and localized just inside (white arrows) the cellular membrane of muHSPCs. By hour 5, most MkMPs are localized inside the murine cells as indicated by the different fluorescent patterns from the stained huMkMPs at different z planes at the same location of murine cells. Several of these stained huMkMPs have released their content

(stained green) into the murine cells: compare the green fluorescent regions within the murine cells at different z planes, e.g., plane 16/38 versus 20/38. These patterns of release of huMkMP green-stained content into target cells resemble the previously-reported patterns of huMkMPcontent release into huHSPCs¹³. We conclude that huMkMPs recognize and are internalized by muHSPCs in an apparently similar fashion that they recognize and are internalized by huHSPCs. Next, to examine if huMkMPs are capable of triggering muHSPCs Mk differentiation as they do for huHSPCs, we carried out huMkMPs/muHSPCs co-cultures (without TPO) for 5 days. Our previous data have shown that, based on our culture protocol, murine Mk cells reach the highest polyploidy state after 4-6 days of *in vitro* culture with TPO^{15,22}. Here, day 5 cells were fixed and stained for beta-tubulin I (TUBB1), von Willebrand factor (vWF), and nucleus (DAPI). As shown in Fig. 2A and Supplemental Figure S1, we identified large Mk cells with strong vWF expression and proplatelets/platelet formation both from huMkMP co-culture and TPO culture. Furthermore, strong CD41 expression was detected on cells using live-cell imaging in huMkMPs co-culture or TPO culture, but not vehicle control (Supplemental Figure S2). Next, we examined muMk maturation via ploidy analysis. The number of total and polyploid (>=8N) Mk cells from the co-culture with huMkMPs increased significantly by 6.8-7.0 fold compared to vehicle control. Notably, while similar numbers of total Mks were produced at day 5 in "huMkMPs" with "TPO" culture (Fig. 2B), muMks from huMkMP-induced culture exhibited less mature characteristics (4-32N) than TPO-induced culture (16-128N) (Fig. 2C). Representative plots of ploidy analysis via flow cytometry are shown in Supplemental Figure S3. Previously, we have shown that huMkMPs were able to induce Mk differentiation and promote cell proliferation of huHSPCs (Figure 5B in Ref.⁴). Similarly, here, our data demonstrate that huMkMPs target and

trigger megakaryocytic differentiation and proliferation of muHSPCs, and proplatelets/platelet production.

Infusion of huMkMPs enhance murine platelet levels in both normal and thrombocytopenic mice

We hypothesized that the *in vitro* biological activity of MkMPs, that is, their ability to target and program muHSPCs towards Mk differentiation, is retained in vivo. To test this hypothesis, we first examined the biological effect of intravenous administration of huMkMPs in healthy wildtype (WT) Balb/c mice. Briefly, two different doses of huMkMPs $(2\times10^6 \text{ or } 6\times10^6)$ were intravenously injected into the mice via the tail vein. 72 hours post huMkMP injection, blood was collected to count the murine platelet concentrations. We chose 72 hours as the blood collection timepoint based on the assumption that three days would be a reasonable period to see the impact of de novo platelet biogenesis from muHSPCs. Upon administration of 2×10⁶ huMkMPs, murine platelet levels were elevated by 18.5% but not in a statistically significantly way (Fig. 3A), but injection of 6×10⁶ huMkMPs significantly elevated murine platelet levels by 26.7% (Fig. 3B). These data (Fig. 3) suggest that huMkMPs target muHSPCs to induce murine Mk differentiation and platelet biogenesis. As an additional control, to exclude the possibility that the effect of huMkMPs on murine platelet counts possibly derives from a secondary reactive thrombocytosis due to the injection of cell membranes, $6x10^6$ Chinese Hamster Ovary (CHO) cell-derived empty membrane vesicles (CHO-MVs) were injected into the Balb/c mice. As shown in Fig. 3C, CHO-MVs did not increase (in fact decreased) platelet levels at 24-hour post injection.

Next, we investigated the potential of huMkMPs in treating murine thrombocytopenia. Based on our previous studies²², mice were intraperitoneally administrated an anti-CD41 antibody (1 µg/g of body weight) to induce thrombocytopenia. Platelet levels drop dramatically within 24 hours and do not fully recover until day 5²². We chose to examine if huMkMPs would ameliorate the drop in platelet concentrations by intravenous administration via the tail vein of 2×10⁶ huMkMPs 8 hours post thrombocytopenia induction. We chose the lower of the two doses examined in the experiments of Fig. 3 for practical reasons, namely the ability to cost- and timeeffectively generate a large enough number of huMkMPs to treat a large cohort of mice. 24 hours post thrombocytopenia induction (the nadir of platelet concentrations with this inducedthrombocytopenia protocol²²), as shown in Fig. 4A, platelet levels dropped 47% in thrombocytopenic mice. Administration of 2×10⁶ huMkMPs into untreated mice significantly increased murine platelet levels by 49% 16 hours post huMkMP administration, while murine platelet levels in thrombocytopenic mice were significantly elevated by 51%, although not restored to the levels of the untreated mice. It was somewhat unexpected that administration of the lower dose of 2×10⁶ huMkMPs into untreated mice would increase murine platelet levels by 49% after 16 hours given the findings of Fig. 3A. This comparison then would suggest that huMkMPs induce murine platelet biogenesis very quickly, and that by 72 hours, the platelet levels appear to be dropping towards homeostatic levels.

To test the hypothesis that huMkMPs induce *de novo* biogenesis of murine platelets (rather than increasing their stability and half-life in circulation), we examined if injection of 2×10^6 huMkMPs into thrombocytopenic or untreated mice would increase the percent of newly synthesized (reticulated) platelets. As shown in Fig. 4B, administration of 2×10^6 MkMPs into untreated mice significantly enhanced the percent of reticulated platelet from the steady-state

level of 11.8% to 15.9%. While the induction of thrombocytopenia increased the level of reticulated platelets to 18.3%, administration of huMkMPs increased the reticulated platelet levels to 19.9%. The data of Fig. 4B support the hypothesis that the observed increases in platelet concentrations are a result of the interaction between huMkMPs and muHSPCs giving rise to newly synthesized murine platelets.

Biodistribution of huMkMPs in the wild-type murine model

To complement our data above, we also investigated the fate of transfused huMkMPs into mice. Briefly, Balb/c mice were intravenously administered 6x10⁶ PKH26-stained huMkMPs or 6x10⁶ PKH26-stained CHO-MVs in filtered PBS via the tail vein. Again, as the properties of the CHO-MV membranes are very distinct from those of huMkMPs, CHO-MVs were used here as a control to huMkMPs for these biodistribution studies. Another control group of mice were administered PBS only. To examine the *in vivo* biodistribution of the PKH26-huMkMPs or PKH26-CHO-MVs, two sets of mice injected with huMkMPs (for collection of tissues at 4 and 24 hours) and one set of mice infused with CHO-MVs (for tissue collection at 24 hours) were sacrificed and the PKH26 signal from various tissue (liver, BM, femurs, blood, spleen, kidney, brain, lungs, and heart) was examined (Fig. 5A). The relative mean fluorescent intensities (MFI) of PKH26 for each tissue are shown in Fig. 5B. PKH26-MFI was greatest in the liver and spleen 4 hour post administration of PKH26-stained huMkMPs. As both of these tissues directly interact with circulating blood, temporary localization of PKH26-stained huMkMPs was expected in these tissues, and thus, this result was expected based on biodistribution data of liposomes administered to Balb/c mice^{23,24}. These findings also mimic the results of other biodistribution studies involving liposomes and nanoparticles, where the liver, kidney, and spleen exhibited the

greatest initial uptake of labeled particles²⁵⁻²⁸. After 24 hours, the relative MFI was reduced in the liver but increased (relative to t=4 hours) in the BM, kidney, lung and heart by 2-5 folds (Fig. 5B), indicating possible target specificity of the huMkMPs. Unlike huMkMPs, CHO-MVs exhibited a different pattern at 24 hours (Fig. 5B), with ~70% of stained CHO-MVs in liver and ~30% in kidney. The biodistribution of the CHO-MVs largely mimicked the patterns exhibited by other membrane vesicles and liposomes in published biodistribution studies²⁵⁻²⁸. These results also suggest that the surface moieties on MkMPs vs those of CHO-MVs play a role in how these vesicles interact with different cells/tissues.

To account for different tissue masses, the MFI of each tissue was normalized by the excised tissue weight. The tissue weight-normalized MFI from huMkMPs-infused group was significantly greater in the BM than any other excised tissue 24 hours after huMkMP administration, except perhaps for spleen and kidney, which were within the margin of significance (p = 0.06) (Fig. 5C). Among all tissues, only the BM demonstrated a large increase in the normalized MFI; the heart exhibited a slight increase in normalized MFI (Fig. 5C). Similar to Fig. 5B, higher normalized-MFI from CHO-MVs was shown in liver, kidney, spleen, and circulating blood (Fig. 5C). Note that storage of tissues in 3 ml of PBS for a few hours before processing would to some extent deplete the tissues of non-adherent blood cells.

Based on the different pattern of biodistribution exhibited by huMkMPs and CHO-MVs (Fig. 5B) and the fast response of *de novo* platelet biogenesis (Fig. 4), we hypothesized that huMkMPs are able to target muHSPCs or more differentiated cells *in vivo*. To examine this hypothesis, $6x10^6$ PKH26-labeled huMkMPs, or saline control were administrated into Balb/c mice. BM, lung, liver and spleen were chosen for examination based on the higher relative PKH26-MFI at 24 hours shown in Fig. 5B. Tissues were collected after 4 hours, stored in 3 mL

PBS and then processed for single-cell isolation and RBC depletion. Harvested single cells were stained with anti-CD41, anti-CD117 or anti-CD45 antibody and analyzed via flow cytometry. Somewhat unexpectedly, in addition to BM, liver, lung and spleen appear to be a reservoir of a good number of CD41⁺ (Mk) cells (Figure 5D), despite the storage (that would remove loosely adherent blood cells) of these tissues in 3 mL PBS prior to processing. For example, almost 20% of the single cells from the processing of the liver tissue from the mice infused with huMkMPs are CD41⁺. One would assume that these are circulating CD41⁺ progenitors and immature Mk cells trapped or retained in the liver. Similarly for the other tissues. Although not statistically significant due to the small number of mice used (n=2), upon huMkMP infusion, the % of CD41⁺ cells generally increased in each tissue, especially in the liver and lung (Figure 5D). Furthermore, we examined the colocalization of signal from the PKH26⁺ huMkMPs and murine HSPC (CD117/c-KIT⁺), CD41⁺ and hematopoietic (CD45⁺) cells in the liver, which had the highest fraction of CD41⁺ cells, thus making data outcomes and their analysis easier and more robust. As shown in the Figure 5E, a significant fraction of CD41⁺ cells were CD41⁺PKH26⁺. This fraction is one fourth (25%) of the CD41⁺ cells in the liver, which was calculated as follows: 5% of single cells from the liver processing were CD41⁺PKH26, while 20% of single cells from the liver processing were CD41⁺ cells (Figure 5D). 5% is one fourth of the 20%. Similarly, there were significant numbers of cells that were CD117⁺PKH26⁺ (ca. 8% of single cells from the liver processing; 45% of the CD117⁺ cells) and CD45⁺PKH26⁺ (2%; 6% of the CD45+ cells). These data indicate that CD117+, CD41+, and generally immature hematopoietic (CD45⁺) cells were targeted by huMkMPs. We were not able to identify colocalization of PKH26 signal with CD41⁺ cells in the BM. This is likely due to the low frequency of CD41⁺ cells in the BM (Figure 5D) and relatively low number of PKH26⁺ huMkMPs in the BM (Figs.

5B & C), thus rendering such colocalization events below the flow-cytometric detection limits, similarly for colocalization of PKH26 signal with CD117⁺ or CD45⁺ cells in the BM.

Nevertheless, these results, and notably the data of Figs. 5D & E, suggest that huMkMPs target CD117⁺, CD41⁺, and CD45⁺ cells (collectively: progenitor cells), and, together with the data of Figs. 5B & C, that the targeting is localized in the liver, lung, BM, and spleen. Liver and lung, emerge then as significant sites of CD41⁺-cell biogenesis upon PKH26⁺ huMkMPs infusion.

Discussion

We demonstrated that, *in vitro*, huMkMPs can target muHSPCs in a way similar to that of targeting huHSPCs (Fig. 1). This targeting induced megakaryocytic differentiation of muHSPCs, and was comparable to TPO-induced differentiation (Fig. 2). We have previously shown that huMkMPs recognize and target huHSPCs via huHSPCs receptors that include CD11b, CD18, CD54 and CD43 ¹³. Based on BLAST analysis, CD11b, CD18, CD54 and CD43 show protein-level conservation between human and murine cells of 86% 90%, 67%, and 59%, respectively. It is possible then that huMkMPs may target muHSPCs using the same receptors. We have also identified two mechanisms of how into huHSPC internalize huMkMPs: membrane fusion and endocytosis¹³. Similar mechanisms may be engaged for the interactions between huMkMPs with muHSPCs.

Based on our *in vitro* studies, we then demonstrated that intravenous administration of huMkMPs into healthy or thrombocytopenic mice resulted in enhanced total platelet levels with newly synthesized platelets after 16-hour post huMkMPs injection (Fig. 4B). It was somewhat surprising that huMkMP can induce *de novo* murine platelet biogenesis so quickly, and this suggested that huMkMP do not only target muHSPCs but also more differentiated cells to induce

megakaryocytic differentiation. This hypothesis is supported by our current finding in Figs. 5D & 5E together with our published finding that huMkMPs target and can induce megakaryocytic differentiation and enhanced survival of day 1 and 3 cultured human CD34⁺ cells⁴. We also demonstrated that, *in vivo*, huMkMPs localize quickly (4 hours) and are highly enriched in the BM, lung, spleen and kidney 24 hours after injection (Fig. 5B & 5C). It has been previously reported that lungs and spleen are important reservoirs of Mk progenitors producing proplatelets/platelets²⁹. Our data suggest that huMkMPs retained in the spleen and lung (Figure 5B & C) may target hematopoietic or Mk progenitors (Fig. 5E) to rapidly induce *de novo* platelet biogenesis. It has been shown that HSPCs are also found in the adult liver³⁰, and although Mk cells could not be detected in the adult liver using 2-photon intravital microscopy (2PIVM),²⁹ given the presence of HSPCs and the production of TPO in liver, Mk cells would be logically expected in the adult liver. Our data (Figs. 5D & E) seem to confirm the presence of muCD41⁺ cells in the adult murine liver, where these and muHSPCs may be targeted by huMkMPs to produce platelets in the liver, as well.

The biological impact of huMkMPs on muHSPCs might be mediated by the delivery of huMkMPs RNA as in the case in huMkMPs targeting huHSPCs ¹³. We have recently reported that two of the most abundant microRNAs (miRs) in huMkMPs, miR-486-5p and miR-22-3p, are likely important in triggering megakaryocytic differentiation in huHSPCs¹⁶. These two miRs are identically conserved on the murine genome ³¹, and their role appears to be conserved as well ³².

Several methods have been explored for delivering therapeutic cargo to specific cells or tissues *in vivo*, but tissue- or cell-specific delivery remains a challenge, particularly for HSPCs³³. Viral vectors have high transfection efficiencies but could be toxic due to insertional mutagenesis, and could elicit an immune response from the host³³. Other carriers, such as

liposomes, have demonstrated effective delivery of cargo to different tissues *in vivo*, but target specificity is only attained by engineering the liposome's surface^{28,34}. Use of EVs addresses some of the shortcomings of liposomes and viral vectors. Wen *et al* have demonstrated the innate targeting ability of intravenously administered 4T1 and 67NR exosomes to target breast-tumor cells *in vivo*.³⁵ Tian *et al*. demonstrated specific targeting cerebral tissue using exosomes²⁸. Similar to our findings, prior studies have reported initial localization of labeled EVs in liver, kidneys, and spleen, with improved tissue-specific targeting occurring after a 24-hour circulation. ^{28,35} However, Tian *et al*. observed significant retention in the liver with extended circulation, with a several-fold increase in liver localization compared to the targeted tissue²⁸. Here, huMkMP localization in the BM was significantly or near significantly higher than all other tissues examined.

As discussed, platelets are an expensive product in limited supply due to limitations in platelet preservation and donor sources⁸. One unit of platelets for transfusion contains $3-4 \times 10^{11}$ platelets and is able to enhance platelet levels by $\sim 10\%$. Wang *et al* showed that culture-derived human platelets, or PLPs, were quickly cleared *in vivo* by macrophages after injection into mice¹². However, infused human Mks were able to produce functional platelets *in vivo* ¹². Our data support the idea of using huMkMPs to induce platelet production *in vivo*. Our study demonstrated that 2×10^6 huMkMPs can increase platelet levels in WT mice by 49% (Fig. 4A) & 27% (Fig. 3B) at 24 and 72 hour, respectively. It is most likely that the effect of huMkMPs on muHSPCs in promoting *de novo* platelet biogenesis is less effective than on huHSPCs. Even so, the platelet boost from 2×10^6 huMkMPs far exceeds the platelet boost in humans from one unit of platelets. In Table 1, we estimate the human equivalent dosage (HED) of MkMPs that would be needed clinically based on FDA guidelines:³⁷

Km is a correction factor defined as the ratio of average body weight to body surface area of the species. The calculated human dosage is 5×10^8 MkMPs for a 60-kilograms adult.

In vivo, Mks can produce between 2,000 and 11,000 platelets but in vitro only few Mk cells can produce platelets and typically 10-100 per Mk. 38-40 With current optimized practices, it is possible to produce 40-50 Mks per input HSPC (CD34⁺ cell).⁴¹ Thus, a single platelet transfusion unit will require almost 10⁸ CD34⁺ cells, which is 50 fold higher than the number contained in a single Umbilical Cord Blood (UCB) collection (2x10⁶), or 50% of a single apheresis of MPB, typically 2x10⁸ CD34⁺ cells. The availability and cost of such large numbers of CD34⁺ cells and the small number of platelets or PLPs generated per CD34⁺ cell limit the scalability and the economic feasibility of platelet manufacturing. If however one focuses on manufacturing MkMPs from cultured Mks, the numbers look quite promising and the process appears both feasible and cost-effective. Table 2 shows calculations of MkMPs yields per input Mk or CD34⁺ cell collected from UCB or MPB, based on current performance metrics including the use of biomechanical forces (shear) to enhance MkMP biogenesis by 47-fold compared to static MkMP production⁴. These calculations suggest that production of therapeutic doses of MkMPs are practical. With process optimization and the development of large-scale EV manufacturing processes⁴², MkMP yields per input CD34⁺ cell would be expected to improve by at least 50- to 100-fold.

Based on these proof-of-concept findings and engineering analyses, huMkMPs appear to hold a good potential to serve as a platelet substitute to ameliorate thrombocytopenias, and to enhance platelet biogenesis in patients with thrombotic deficiency. In view of the fact that huMkMPs can be stored frozen ¹³, such a MkMP product could also resolve the issue of

availability on demand at any location worldwide. Furthermore, based on our recent data¹⁶ showing that, *in vitro*, MkMPs can be used to effectively deliver exogenously loaded plasmid DNA and small RNAs to huHSPCs, our data here demonstrating *in vivo* effectiveness of huMkMPs in targeting HSPCs would open up the possibility of using modified MkMPs for gene therapy applications to address hematologic abnormalities.

Acknowledgements

We thank Jeff Caplan and members of Bioimaging Center (Univ. of Delaware) for assistance with Confocal Microscopy.

This project was supported by a grant (CBET-1804741) by the US National Science Foundation.

Authorship Contributions

E.T.P., C.E., CY.K., and S.D. designed the study and analyzed the data; C.E., CY.K. and S.D. carried out the experiments. E.T.P., CY.K. and S.D. wrote the manuscript.

Disclosure of Conflict-of-interest: E.T.P and C.Y.K. are listed as inventors on a pending US/PCT patent application (publication US20170058262A1, Application No. 15/308,221, PCT No. PCT/US15/31388) on MkMP-based technologies. The rights to the pending patent belong to the three inventors of the patent.

References:

- 1. Patel-Hett S, Wang H, Begonja AJ, et al. The spectrin-based membrane skeleton stabilizes mouse megakaryocyte membrane systems and is essential for proplatelet and platelet formation. *Blood*. 2011;118(6):1641-1652.
- 2. Machlus KR, Italiano JE, Jr. The incredible journey: From megakaryocyte development to platelet formation. *J Cell Biol*. 2013;201(6):785-796.
- 3. Patel SR, Hartwig JH, Italiano JE, Jr. The biogenesis of platelets from megakaryocyte proplatelets. *J Clin Invest*. 2005;115(12):3348-3354.
- 4. Jiang J, Woulfe DS, Papoutsakis ET. Shear enhances thrombopoiesis and formation of microparticles that induce megakaryocytic differentiation of stem cells. *Blood*. 2014;124(13):2094-2103.
- 5. Flaumenhaft R, Dilks JR, Richardson J, et al. Megakaryocyte-derived microparticles: direct visualization and distinction from platelet-derived microparticles. *Blood*. 2009;113(5):1112-1121.
- 6. Agrahari V, Agrahari V, Burnouf PA, Chew CH, Burnouf T. Extracellular Microvesicles as New Industrial Therapeutic Frontiers. *Trends Biotechnol*. 2019;37(7):707-729.
- 7. Panfoli I, Santucci L, Bruschi M, et al. Microvesicles as promising biological tools for diagnosis and therapy. *Expert Rev Proteomics*. 2018;15(10):801-808.
- 8. Stroncek DF, Rebulla P. Platelet transfusions. *Lancet*. 2007;370(9585):427-438.
- 9. Levy JH, Neal MD, Herman JH. Bacterial contamination of platelets for transfusion: strategies for prevention. *Crit Care*. 2018;22(1):271.
- 10. Reems JA, Pineault N, Sun SJ. In Vitro Megakaryocyte Production and Platelet Biogenesis: State of the Art. *Transfusion Medicine Reviews*. 2010;24(1):33-43.
- 11. Lambert MP, Sullivan SK, Fuentes R, French DL, Poncz M. Challenges and promises for the development of donor-independent platelet transfusions. *Blood*. 2013;121(17):3319-3324.
- 12. Wang Y, Hayes V, Jarocha D, et al. Comparative analysis of human ex vivo-generated platelets vs megakaryocyte-generated platelets in mice: a cautionary tale. *Blood*. 2015;125(23):3627-3636.
- 13. Jiang J, Kao CY, Papoutsakis ET. How do megakaryocytic microparticles target and deliver cargo to alter the fate of hematopoietic stem cells? *J Control Release*. 2017;247:1-18.
- 14. Alvarez LL, Pardo HG. Guide for the care and use of laboratory animals Natl-Res-Council. *Psicothema*. 1997;9(1):232-234.
- 15. Fuhrken PG, Apostolidis PA, Lindsey S, Miller WM, Papoutsakis ET. Tumor suppressor protein p53 regulates megakaryocytic polyploidization and apoptosis. *J Biol Chem*. 2008;283(23):15589-15600.
- 16. Kao CY, Papoutsakis ET. Engineering human megakaryocytic microparticles for targeted delivery of nucleic acids to hematopoietic stem and progenitor cells. *Sci Adv.* 2018;4:eaau6762
- 17. Gupta N, Patel B, Ahsan F. Nano-engineered erythrocyte ghosts as inhalational carriers for delivery of fasudil: preparation and characterization. *Pharm Res.* 2014;31(6):1553-1565.
- 18. Fang RH, Hu CM, Luk BT, et al. Cancer cell membrane-coated nanoparticles for anticancer vaccination and drug delivery. *Nano Lett.* 2014;14(4):2181-2188.

- 19. Chiu J, Valente KN, Levy NE, Min L, Lenhoff AM, Lee KH. Knockout of a difficult-to-remove CHO host cell protein, lipoprotein lipase, for improved polysorbate stability in monoclonal antibody formulations. *Biotechnology and Bioengineering*. 2017;114(5):1006-1015.
- 20. Bogue MA, Grubb SC, Walton DO, et al. Mouse Phenome Database: an integrative database and analysis suite for curated empirical phenotype data from laboratory mice. *Nucleic Acids Res.* 2018;46(D1):D843-D850.
- 21. Freshney RI. Culture of animal cells: A manual of basic technique and specialized applications. Hoboken, NJ: Wiley; 2016.
- 22. Apostolidis PA, Woulfe DS, Chavez M, Miller WM, Papoutsakis ET. Role of tumor suppressor p53 in megakaryopoiesis and platelet function. *Exp Hematol*. 2012;40(2):131-142 e134.
- 23. Thierry AR, Lunardi-Iskandar Y, Bryant JL, Rabinovich P, Gallo RC, Mahan LC. Systemic gene therapy: biodistribution and long-term expression of a transgene in mice. *Proc Natl Acad Sci U S A*. 1995;92(21):9742-9746.
- 24. Connor J, Norley N, Huang L. Biodistribution of pH-sensitive immunoliposomes. *Biochim Biophys Acta*. 1986;884(3):474-481.
- 25. Bartneck M, Scheyda KM, Warzecha KT, et al. Fluorescent cell-traceable dexamethasone-loaded liposomes for the treatment of inflammatory liver diseases. *Biomaterials*. 2015;37:367-382.
- 26. Xie G, Sun J, Zhong G, Shi L, Zhang D. Biodistribution and toxicity of intravenously administered silica nanoparticles in mice. *Arch Toxicol*. 2010;84(3):183-190.
- 27. Yu B, Hsu SH, Zhou C, et al. Lipid nanoparticles for hepatic delivery of small interfering RNA. *Biomaterials*. 2012;33(25):5924-5934.
- 28. Tian T, Zhang HX, He CP, et al. Surface functionalized exosomes as targeted drug delivery vehicles for cerebral ischemia therapy. *Biomaterials*. 2018;150:137-149.
- 29. Lefrancais E, Ortiz-Munoz G, Caudrillier A, et al. The lung is a site of platelet biogenesis and a reservoir for haematopoietic progenitors. *Nature*. 2017;544(7648):105-109.
- 30. Taniguchi H, Toyoshima T, Fukao K, Nakauchi H. Presence of hematopoietic stem cells in the adult liver. *Nature Medicine*. 1996;2(2):198-203.
- 31. Kozomara A, Birgaoanu M, Griffiths-Jones S. miRBase: from microRNA sequences to function. *Nucleic Acids Res.* 2019;47(D1):D155-D162.
- 32. Wong N, Wang X. miRDB: an online resource for microRNA target prediction and functional annotations. *Nucleic Acids Res.* 2015;43(Database issue):D146-152.
- 33. Yu KR, Natanson H, Dunbar CE. Gene Editing of Human Hematopoietic Stem and Progenitor Cells: Promise and Potential Hurdles. *Hum Gene Ther*. 2016;27(10):729-740.
- 34. Johnsen KB, Gudbergsson JM, Skov MN, Pilgaard L, Moos T, Duroux M. A comprehensive overview of exosomes as drug delivery vehicles endogenous nanocarriers for targeted cancer therapy. *Biochim Biophys Acta*. 2014;1846(1):75-87.
- 35. Wen SW, Sceneay J, Lima LG, et al. The Biodistribution and Immune Suppressive Effects of Breast Cancer-Derived Exosomes. *Cancer Res.* 2016;76(23):6816-6827.
- 36. Kaufman RM, Djulbegovic B, Gernsheimer T, et al. Platelet transfusion: a clinical practice guideline from the AABB. *Ann Intern Med.* 2015;162(3):205-213.
- 37. Nair AB, Jacob S. A simple practice guide for dose conversion between animals and human. *J Basic Clin Pharm*. 2016;7(2):27-31.

- 38. Cho J. A paradigm shift in platelet transfusion therapy. *Blood*. 2015;125(23):3523-3525.
- 39. Kim AR, Sankaran VG. Development of autologous blood cell therapies. *Experimental Hematology*. 2016;44(10):887-894.
- 40. Thon JN, Mazutis L, Wu S, et al. Platelet bioreactor-on-a-chip. *Blood*. 2014;124(12):1857-1867.
- 41. Panuganti S, Schlinker AC, Lindholm PF, Papoutsakis ET, Miller WM. Three-stage ex vivo expansion of high-ploidy megakaryocytic cells: toward large-scale platelet production. *Tissue Eng Part A*. 2013;19(7-8):998-1014.
- 42. Kao C-Y, Papoutsakis ET. Extracellular vesicles: exosomes, microparticles, their parts, and their targets to enable their biomanufacturing and clinical applications. *Current opinion in biotechnology*. 2019;60:89-98.

Tables

Table 1. Conversion of MkMP dosage from mouse to human

	Mouse	Human
Body Weight (kg)	0.0184	60
Body Surface Area (cm ²)	0.007	1.62
Km (kg/cm ²)	2.8	37
MkMPs needed for transfusion	2 × 10 ⁶	5 × 10 ⁸

Table 2. MkMP yield from static or stimulated-culture

MkMP	Static	Biomech. Force
Yield (per Mk)	1	47
Yield (per CD34 ⁺ Cell)	45	2115
# per CD34 ⁺ cell collection from UCB (2x10 ⁶) or PB (2x10 ⁸)	9 × 10 ⁷⁻⁹	4 × 10 ⁹⁻¹¹

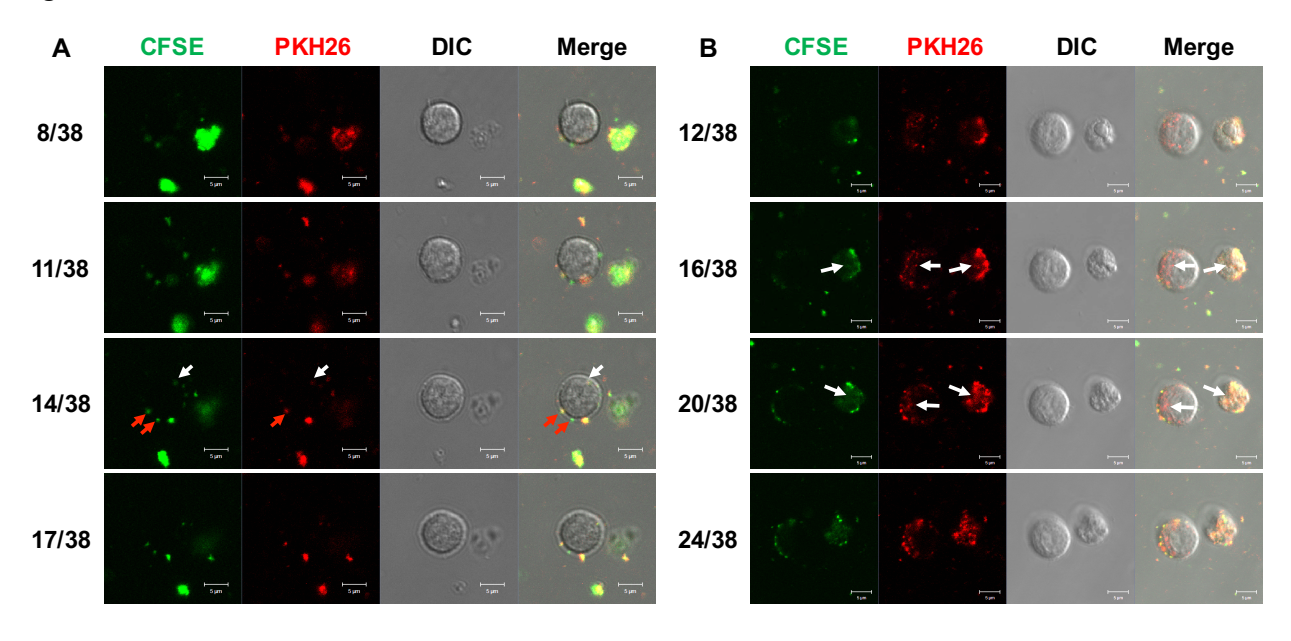
Figure Legends

- **Figure 1. Co-culture of huMkMPs and muHSPCs** *in vitro*. muHSPCs were co-cultured for up to 5 hours with huMkMPs stained with CFSE and PKH26. Cells were examined by confocal microscopy at (A) 3 hours or (B) 5 hours post co-culture setup, and fluorescent images were taken at different confocal planes. The numbers represent the specific slice number (left) and the total number of slices (right). Red arrows point to huMkMPs binding to muHSPCs, while white arrows point to huMkMPs that have been internalized by muHSPCs.
- Figure 2. Co-culture of huMkMPs and muHSPCs promotes murine megakaryopoiesis. 60,000 muHSPCs were co-cultured with either huMkMPs only, or 50 ng/ml thrombopoietin (TPO), or without any supplements (vehicle control) for 5 days. Cells were harvested and fixed at day 5, and (A) stained for expression of von Willebrand Factor (vWF), beta-tubulin I (TUBB1), and nucleus (DAPI), via confocal microscopy, and also bright-field imaging. (B) Some cells were analyzed by flow cytometry for counting Mk cells, or (C) to measure Mk-cell distribution in various ploidy classes. Scale bar = $10 \mu m$. Error bars represent the standard error of the mean (n=4).
- Figure 3. Intravenous administration of huMkMPs increases *in vivo* platelet concentrations in a wild-type mice 72 hours post administration. (A) 2×10^6 or (B) 6×10^6 huMkMPs were administered intravenously into wild-type Balb/c mice via the tail vein. Murine platelet levels of control mice (untreated) or mice treated with MkMPs were measured 72 hour post huMkMP injection. (C) 6×10^6 huMkMPs (n=8) or 6×10^6 CHO-MVs (n=2), or saline control (n=10) were administered intravenously into wild-type mice via the tail vein, and murine platelet numbers were measured at 24 hours. Error bars represent the standard error of the mean. **, P<0.01
- **Figure 4. Intravenous administration of 2×10**6 huMkMPs into untreated wild-type mice increases murine platelet concentrations and ameliorates thrombocytopenia in thrombocytopenic mice 16 hours post administration. Thrombocytopenia (TP) was induced by intraperitoneal administration of anti-CD41 antibody. After 8 hours, 2×106 huMkMPs were administered intravenously into untreated or thrombocytopenic mice via the tail vein. (A) Murine platelet levels were measured 24 hours post antibody injection (16 hours post huMkMP administration) of untreated (n=7), or mice treated with huMkMPs (n=5), thrombocytopenic mice (n=9), or thrombocytopenic mice treated with MkMPs (n=8). (B) Reticulated (newly synthesized) platelet numbers were measured 24 hours post antibody injection (16 hours post huMkMP administration) by flow cytometry for a subset of mice in the four murine cohorts of panel A, and the data are presented as % of the total platelet count. Error bars represent the standard error of the mean. *, P<0.05, **, P<0.01, *** P<0.001
- Figure 5. *In vivo* biodistribution of administered PKH26-labeled huMkMPs in untreated wild-type mice and huMkMP colocalization with murine blood cells. Murine tissues were excised, homogenized, and analyzed for fluorescence (SpectraMax i3x) 4 and 24 hours after huMkMPs or CHO-MVs administration. (A) Experimental schema for measuring tissue-specific fluorescence. (B) Mean fluorescence intensity (MFI) in each excised tissue relative to total fluorescence in all tissues (n=6 mice per MkMP group, n=3 mice in CHO-MV group). (C) MFI

of each tissue per g excised tissue. (D) $6x10^6$ PKH26-labeled huMkMPs, or saline control were administered into Balb/c mice. Tissues, including BM, lung, liver, and spleen were collected after 4 hours for single-cell isolation. Harvested cells were stained with anti-CD41 antibody and analyzed via flow cytometry (n=2). (E) Single cells isolated from the liver were analyzed by flow cytometry for colocalization of PKH26 signal with CD41, CD117, or CD45 signals (n=2). Error bars represent the standard error of the mean. Unpaired 2-tailed t test was used to determine statistical significance. *P < 0.05. Higher P values of some comparisons are displayed over the bars.

Figures

Figure 1





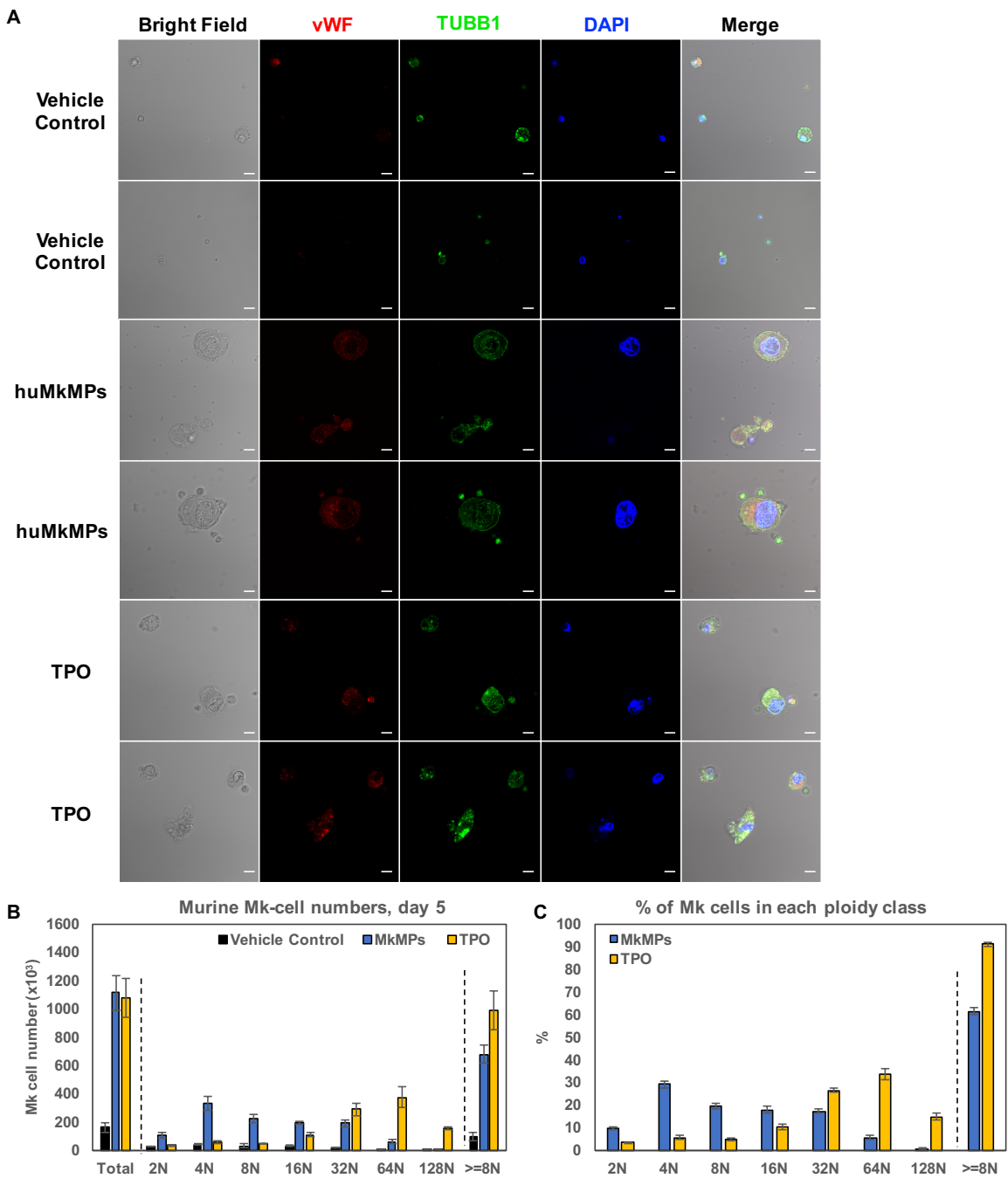


Figure 3

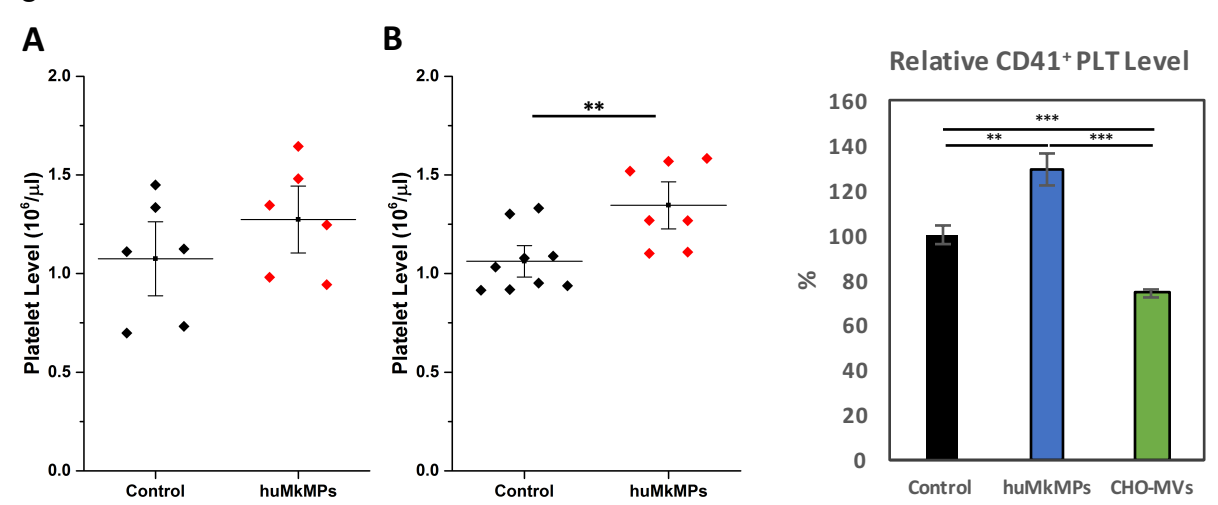


Figure 4

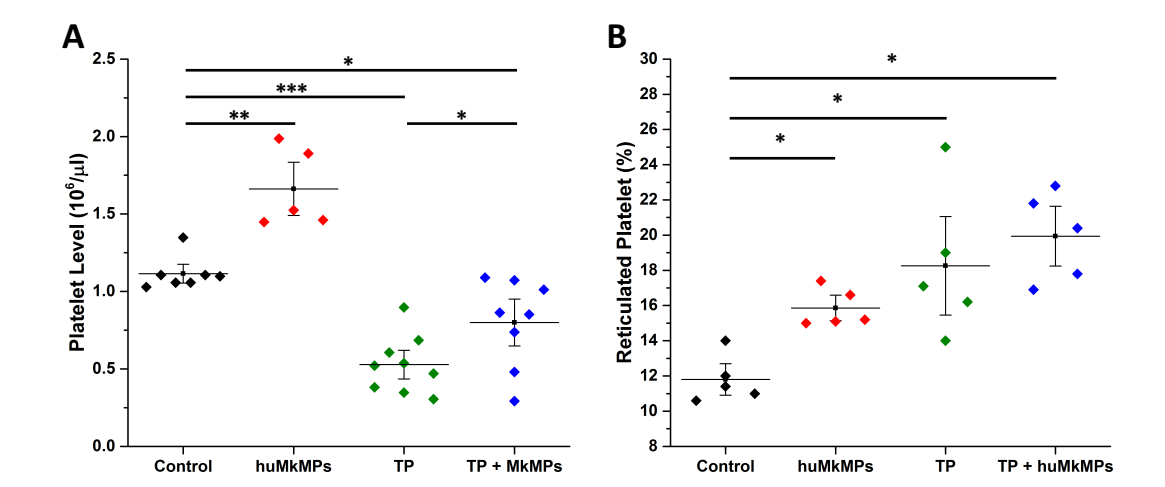


Figure 5

